

# A molecular dynamics study on surface properties of supercooled water

LÜ Yongjun & WEI Bingbo

Department of Applied Physics, Northwestern Polytechnical University, Xi'an 710072, China

Correspondence should be addressed to Wei Bingbo (email: [bbwei@nwpu.edu.cn](mailto:bbwei@nwpu.edu.cn))

Received May 10, 2005; accepted July 14, 2006

**Abstract** Molecular dynamics simulations were performed to study the surface properties of water in a temperature range from 228 to 293 K by using the extended simple point charge (SPC/E) and four-site TIP4P potentials. The calculated surface tension increases with the decrease of temperature, and moreover the slopes of the surface tension-temperature curves show a weak rise below 273 K, whereas no obvious anomalies appear near 228 K, which accords with the previous experiments. Compared with the measured values, the SPC/E potential shows a good agreement, and the TIP4P potential underestimates the surface tension. The main reason for that may be the reasonable description of the surface structure of supercooled water for the SPC/E. When simulating the orientational distributions of water molecules near the surface, the SPC/E potential produces higher ordering and larger surface potentials than the TIP4P potential.

**Keywords:** surface tension, supercooled water, molecular dynamics simulation.

Liquid-vapor interface has aroused wide research interest in experimental and theoretical fields in recent several years because of its importance in physics, biology and environmental science<sup>[1–5]</sup>. As a transition phase between the two bulk systems, liquid-vapor interface displays different physical and chemical properties. In particular, water, the most popular liquid in nature, has especially large surface tension compared to some simple liquids owing to the hydrogen-bonding structure at the surface. Therefore, the better understanding of thermodynamic and dynamic properties associated with liquid-vapor interface requires a molecular-level investigation of surface structure.

Molecular dynamics (MD) simulation is one of the effective methods to study interfacial phenomena in molecular level<sup>[6]</sup>. In the past decade, the surface properties of water have been subjected to extensive investigation by MD method using various interaction potentials<sup>[7–9]</sup>. Guissani and Guillot studied the liquid-vapor coexistence curve of SPC/E water and discussed the relationship between the structural change of water molecules and the slope of the liquid-vapor coexistence curve<sup>[7]</sup>. Wilson *et al.* simulated the surface tension and surface potential of water at 325 K for the TIP4P model<sup>[8]</sup>. The corrected

value of the surface tension is  $59 \text{ mNm}^{-1}$ , which is 13% smaller than the experimental results. And the calculated surface potential has reasonable magnitude but opposite sign. Alejandro *et al.*<sup>[9]</sup> investigated the liquid-vapor equilibrium of water in the range of 316–573 K by using the SPC/E model with the Ewald sum. The simulated surface tensions are in good agreement with the experimental results, which suggests that the SPC/E model is a more effective potential function for studying the liquid-vapor interface of water.

It is noted that most studies on the surface properties of water concentrate on high temperature region, and less attention is paid to supercooled water. Although Matsumoto and Kataoka<sup>[10]</sup> studied the surface properties of water in a wide temperature range from 250 to 400 K with MD method, including surface tension, surface excess energy and orientational structure near the surface, the simulated surface tensions are 50% smaller than the experimental values, and moreover, the specific surface entropy  $s_s$  ( $s_s = -d\gamma/dT$ ,  $\gamma$  is the surface tension,  $T$  the temperature) diminishes monotonously with the decrease of temperature in the supercooled region, which is contradictory to the experimental results by Floriano *et al.*<sup>[11]</sup>. Floriano *et al.*<sup>[11]</sup> measured the surface tension of water using a small-sample capillary rise method down to 245.8 K and the results showed that  $s_s$  is inclined to increase below 273 K. Therefore, it is necessary to investigate the surface tension of supercooled water in detail.

In this paper, we report a study on the surface properties of supercooled water down to 228 K with a classical MD method, and the behaviors of the surface tension and surface structure in the supercooled region are discussed.

## 1 Simulation method

During the simulations, the SPC/E and 4-site TIP4P potential functions are utilized. The interaction between two water molecules is a combination of Lennard-Jones 6-12 potential function and Coulomb potential:

$$U(r_{ij}) = 4\varepsilon_{ij} \left[ \left( \frac{\sigma_{ij}}{r_{ij}} \right)^{12} - \left( \frac{\sigma_{ij}}{r_{ij}} \right)^6 \right] + \frac{q_i q_j}{r_{ij}}, \quad (1)$$

where  $r_{ij}$  is the distance between atom  $i$  and  $j$  in two different molecules;  $q_i$  and  $q_j$  are the charges of atom  $i$  and  $j$ ;  $\varepsilon_{ij}$  and  $\sigma_{ij}$  are Lennard-Jones parameters. The potential parameters for the SPC/E and TIP4P models are given in Table 1.

Table 1 Molecular potential parameters for the SPC/E and TIP4P potential functions<sup>[12,13]</sup>

	SPC/E	TIP4P
$r_{\text{O-H}} (\text{\AA})$	1.0	0.9572
$\angle \text{HOH} (\text{deg})$	109.47	104.52
$\sigma (\text{\AA})$	3.166	3.154
$\varepsilon (\text{kJ}\cdot\text{mol}^{-1})$	0.6502	0.6481
$q_{\text{O}} (e)$	-0.8746	0
$q_{\text{H}} (e)$	0.4238	0.52
$q_{\text{M}} (e)$	0	-1.04
$r_{\text{O-M}} (\text{\AA})$	0	0.15

The simulation domain is schematically shown in Fig. 1. Periodical boundary conditions are applied in the three coordinate directions. The simulation system consists of 512 water molecules. The simulation is performed with a time step of 2.5 fs, and the simulation temperature ranges from 228 to 293 K. The short-range potential cutoff is 9.8 Å. At each temperature, the bulk water system without liquid-vapor interface is equilibrated at first and then the  $z$  dimension of the simulation cell is increased to 100 Å in order to form two liquid-vapor interfaces. The new system is equilibrated in a NVT ensemble ranging from  $10^5$  to  $5 \times 10^5$  time steps with the decrease of simulation temperature. The production runs of  $10^5$  time steps are required to calculate the surface properties accurately. All of the codes run in HP-rx2600 system at Center for High Performance Computation of NPU.

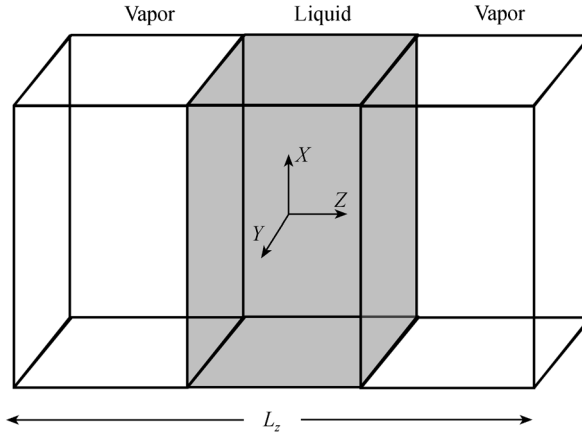


Fig. 1. Simulation cell.  $L_z = 100$  Å for  $N = 512$ . The middle part is liquid water and vapor phase is fixed in each side.

In the MD simulations of dipolar fluids such as water, the long-range electrostatic interactions play an important role and cannot be neglected. Therefore, the Coulomb potential consists of two parts: short-range and long-range forces. The Ewald sum is an effective way to calculate the ionic interaction and it can embody the long-range force in a simulation with periodic boundaries<sup>[14]</sup>. By means of the Ewald sum, the total Coulomb potential  $U_{\text{Coul}}$  is given by

$$U_{\text{Coul}} = \frac{2\pi}{V} \sum_{h \neq 0} \frac{1}{h^2} \exp\left(-\frac{h^2}{4\kappa^2}\right) |S(h)|^2 + \frac{1}{2} \sum_i \sum_a \sum_{j \neq i} q_{ia} \sum_b q_{jb} \frac{\text{erfc}(\kappa r_{iajb})}{r_{iajb}} - \frac{\kappa}{\sqrt{\pi}} \sum_i \sum_a q_{ia}^2 - \frac{1}{2} \sum_i \sum_a \sum_{b \neq a} q_{ia} q_{ib} \frac{\text{erf}(\kappa r_{iaib})}{r_{iaib}}, \quad (2)$$

where  $V$  is the volume of simulation cell,  $h$  the reciprocal lattice vector,  $\kappa (= 5.6/L_x)$  the convergence factor,  $\text{erfc}(x)$  the complementary error function,  $S(h) = \sum_i \sum_a q_{ia} \exp(ih \cdot r_{ia})$

and  $r_{iajb} = r_{ia} - r_{jb}$ . In the simulations, a cutoff is also imposed on the  $h$ -space, and the maximum reciprocal lattice vectors are given by  $|h_x^{\max}| = |h_y^{\max}| = 5$ . Because the size of

simulation cell in the  $z$ -direction is lengthened, the maximum of  $|h_z^{\max}|$  should be increased accordingly and is equal to 15 in this work.

## 2 Results and discussion

### 2.1 Density profiles

In order to observe the formation of liquid-vapor interface, the distribution of number density along  $z$  coordinate is calculated. The simulation cell is divided into slabs with  $0.25 \text{ \AA}$  thickness, and molecule number is statistically averaged in each slab. The density profiles at 293 K and 233 K for the SPC/E and TIP4P potentials are shown in Fig. 2(a) and (b) respectively. There exists obviously a continuous density drop between the bulk liquid and vapor phases, indicating that the liquid-vapor interface forms. The density profiles at every temperature are found to fluctuate around the bulk density. The amplitude of this fluctuation reaches a maximum at the liquid/vapor interface and then falls into oscillations with a weak decay in liquid region. Moreover, the fluctuation becomes more and more pronounced with the decrease of temperature, as shown in the insets of Fig. 2. The oscillatory density profile is a result of surface layering structure which is often observed in some liquids with low melting point and regarded as a simple geometrical re-

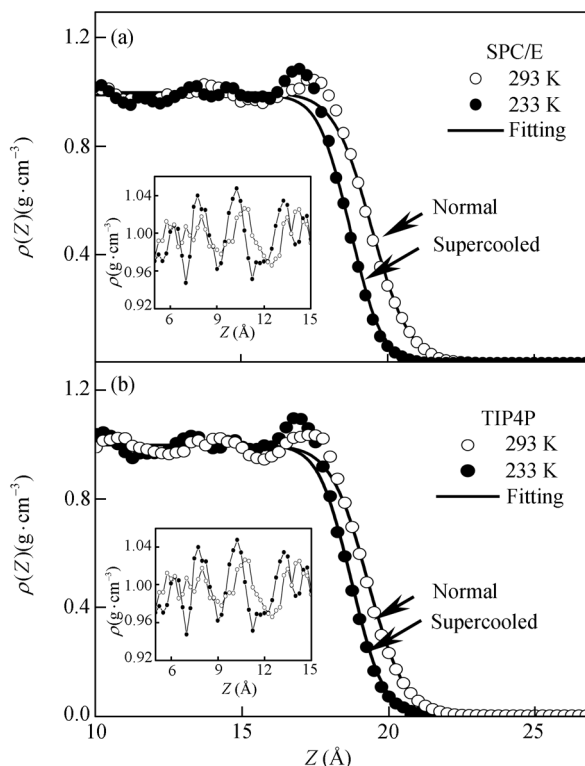


Fig. 2. Density profiles at 293 K (open circles) and 233 K (dots) for the SPC/E and TIP4P potentials. The solid lines are the fitting results according to the hyperbolic tangent function. The insets show the enlargement of liquid density profiles.

sponse to a sharp interface with a short-range correlation. At the free liquid surface, the capillary wave associated with the long-range correlation often suppresses the inhomogeneity of density profile and damps the oscillation. Its effect on the surface layering depends on the transverse size. In simulations, the transverse size of the simulation cell is very small and the effect of capillary waves is often ignored. In fact, according to the analyses of Tarazona *et al.* [15] the layering structure is independent of temperature, and the temperature dependence of the oscillatory density profiles shown in this simulation is caused by the capillary wave essentially. The effect of temperature on the oscillatory amplitude  $A_m$  is described by means of the transverse size  $L_x$ :  $A_m \sim L_x^{-\eta(T,\gamma)}$  ( $\eta$  is the decay exponent, a function of temperature and surface tension). Therefore, the increase of the interface area ( $L_x \times L_y$ ) can damp the density oscillation to a certain extent, but it may not be pronounced in view of the limitation of the typical scope in the present simulations.

The density profiles are fitted by a hyperbolic tangent function:

$$\rho(z) = \frac{1}{2}(\rho_L + \rho_V) - \frac{1}{2}(\rho_L - \rho_V) \tanh[(z - z_0)/d], \quad (3)$$

where  $\rho_L$  and  $\rho_V$  are bulk densities of liquid and vapor phase,  $z_0$  is the position of the Gibbs surface, and  $d$  is a parameter of surface thickness. The fitted  $\rho(z)$  is shown as solid lines in Fig. 2.

The surface thickness  $t$ , defined as the “10–90 thickness”, is a function of  $d$ ,  $t = 2.1972d$ . For both the SPC/E and TIP4P potentials, the surface thickness decreases with the decrease of temperature as shown in Fig. 3. Moreover, in the simulation temperature range, the surface thickness for the TIP4P is about 5% larger than the SPC/E potential. According to Schwartz’s measurements [16], the surface thickness of water reaches 7.2 Å at 293 K, much larger than the values of 2.3 and 2.4 Å obtained in this work. The difference between the simulations and experiments is attributed to the surface capillary waves involved in the experimental measurements. The present results for the SPC/E model is also smaller than that of Matsumoto *et al.* for the CC potential [10], which may relate to the molecular structures defined by these potential functions. The CC and TIP4P potentials

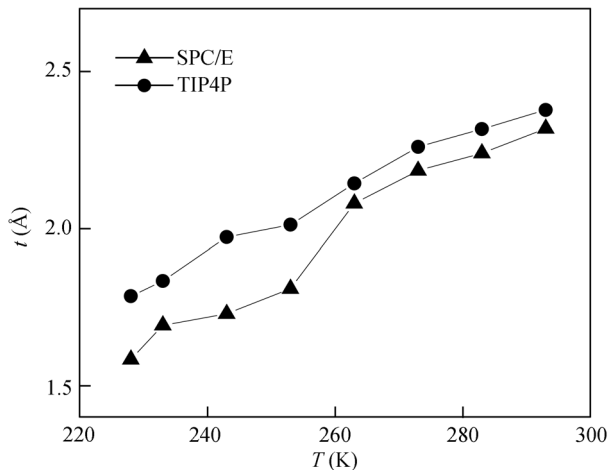


Fig. 3. “10–90 thickness” as a function of temperature for the SPC/E and TIP4P potential functions.

yield weaker interaction force, smaller liquid densities and higher vapor densities, resulting in the larger surface thickness.

## 2.2 Surface tension

Surface tension is one of the important parameters to characterize the surface structure and chemical activity and associates closely with some surface anomalies. In order to understand quantitatively the surface properties of water in the supercooled region, we simulated the surface tension of water as a function of temperature from 228 to 293 K.

The surface tension can be obtained by calculating the components of the pressure tensor<sup>[17]</sup>:

$$\gamma = \frac{A}{2} \left\langle \frac{1}{2} (P_{xx} + P_{yy}) - P_{zz} \right\rangle, \quad (4)$$

where  $P_{xx}$ ,  $P_{yy}$  and  $P_{zz}$  are the  $X$ ,  $Y$  and  $Z$  element of the pressure tensor, and  $A = L_x L_y$  is surface area. The element of the molecular pressure tensor is

$$VP_{\alpha\beta} = \sum_{i=1}^N m_i (v_i)_\alpha (v_i)_\beta + \sum_{i=1}^{N-1} \sum_{j>i}^N \sum_{a,b=1}^u (r_{ij})_\alpha (f_{ijb})_\beta, \quad (5)$$

where  $N$  is the number of molecules;  $m_i$ ,  $v_i$  are the molecular mass and the velocity of the center of mass;  $u$  the number of sites in a water molecule;  $r_{ij}$  the distance between the molecules  $i$  and  $j$ ; and  $f$  the force between atom  $a$  in molecule  $i$  and atom  $b$  in molecule  $j$ . The electrostatic long range interactions make an important contribution to the surface tension and are involved by using the Ewald sum in the simulations based on eq. (2). The tail correction to the surface tension is also performed.

The surface tensions of supercooled water as a function of temperature for the SPC/E and TIP4P models are shown in Fig. 4. The open circles are the measured values by Floriano *et al.*<sup>[11]</sup>; and the solid lines are the best fit for the simulated results. The experimental data above 273 K have been measured extensively and can be accurately fitted by Vargaftik equation<sup>[18]</sup>:

$$\gamma = B \left[ \frac{T_c - T}{T_c} \right]^\lambda \left[ 1 + b \left( \frac{T_c - T}{T_c} \right) \right], \quad (6)$$

where  $T_c = 647.15$  K,  $B = 0.2358$  mNm<sup>-1</sup>,  $\lambda = 1.256$  and  $b = -0.625$ . In general, the surface tension in the supercooled region is obtained approximately from the extrapolation of eq. (6), shown as the dashed line in Fig. 4. It can be seen that the absolute values of the slope of temperature-surface tension curve diminish as the temperature decreases. However, the experimental data given by Floriano display that the temperature dependence of the surface tension begins to increase below 273 K. For the present simulated results, the surface tensions are in good agreement with the measured values in the supercooled state for the SPC/E potential, and are somewhat smaller while  $T > 273$  K. Once the temperature decreases below 273 K, the temperature dependence of the surface tension starts to slowly rise and the specific surface entropy,  $s_s$ , correspondingly increases with the decrease of temperature, as plotted in Fig. 4, which is more evident for the TIP4P potential. This change tendency agrees qualitatively with the experimental results and is contrary to

Matsumoto and Kataoka's results. It is suggested that there may be a second inflection point in the surface tension-temperature curve in the low temperature region as the first one at about 200°C<sup>[19]</sup>. Although the present results show that the temperature dependence of the surface tension is strengthened below 273 K, the increase appears so slow that we cannot confirm the location of the inflection point from the relatively smaller simulation data. And the more extensive simulations in a wide temperature range, especially at larger supercooling, are required.

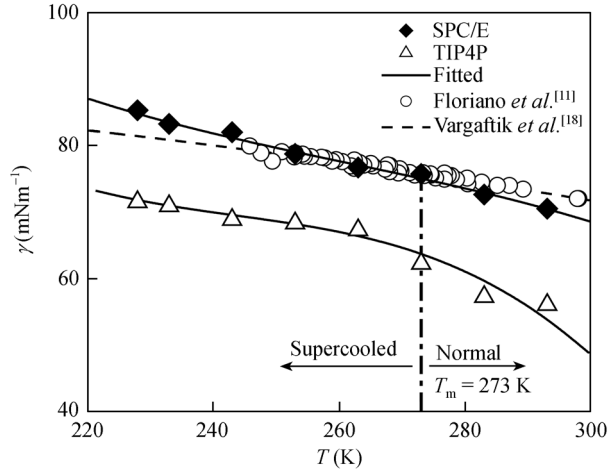


Fig. 4. Surface tension of supercooled water. The solid diamonds and open triangles are calculated values with the SPC/E and TIP4P potentials, respectively. The open circles are measured results in ref. [11]. The solid curves are the best fit to the simulated results. The dash line is the prediction of Vargaftik equation.

In addition, no anomalous behavior of the surface tension like some bulk properties of supercooled water appears when the temperature approaches 228 K<sup>[20]</sup>. Floriano<sup>[11]</sup> explained that the divergence of the surface free energy per mole,  $\gamma V_m^{2/3}$ , at 228 K is mainly caused by the mole volume  $V_m$ , independent of  $\gamma$ . However, it is near 228 K that the anomalous behavior of  $\gamma V_m^{2/3}$  appears, and if the behavior of the surface tension is unknown at 228 K, the above interpretation looks inadequate. The present simulations provide a complete picture of the surface tension near 228 K and can more rigorously elucidate this question.

The comparison of the surface tension between the SPC/E and TIP4P potentials demonstrates that the SPC/E potential is a better model for reproducing the surface characteristics of water in the supercooled state. Considering a good agreement with the experimental values in Alejandre's simulation<sup>[9]</sup> up to the triple point, the SPC/E potential can quantitatively represent the surface tension of water over a wide temperature range.

### 2.3 Orientational structure and surface potential

The orientation of water molecules is determined by two angles  $\theta$  and  $\phi$  according to the definition of Matsumoto *et al.*<sup>[10]</sup>.  $\theta$  is the angle between the surface normal vector  $n_z$

and molecular dipole, and  $\phi$  is the rotational angle around the molecular dipole. It is found that there are preferential orientation angles for SPC/E and TIP4P water molecules near the surface. The statistical averages of the two angles in the liquid side,  $\langle\theta\rangle$  and  $\langle\phi\rangle$ , are  $103^\circ$  and  $62^\circ$  at 293 K for the SPC/E potential. In the vapor side,  $\langle\theta\rangle$  and  $\langle\phi\rangle$  are  $75^\circ$  and  $37^\circ$  respectively. It can be seen that the dipole of water molecules in the liquid side points to the bulk liquid and one hydrogen atom of the molecule projects towards the liquid phase. On the other hand, the molecular dipole in the vapor side prefers to point to the bulk vapor, and one hydrogen atom projects towards the vapor phase. Moreover, these angles are independent of temperature in the simulations. For the TIP4P potential, the values of  $\langle\theta\rangle$  and  $\langle\phi\rangle$  are smaller than that for the SPC/E potential,  $95^\circ$  and  $54^\circ$  in the liquid side,  $84^\circ$  and  $38^\circ$  in the vapor side respectively. Clearly, the degree of orientation ordering of SPC/E water molecules near the surface is higher, which determines stronger surface polarity of water.

The surface potential  $\chi$  is defined as the difference of the electrostatic potential between the bulk liquid and vapor phases. It is calculated according to the following relation:

$$\chi = \frac{\mu}{\epsilon_0} \int_{-\infty}^{\infty} dz \rho(z) \langle \cos \theta \rangle, \quad (7)$$

where  $\mu$  is the dipole moment of water molecules, equal to 2.351D for SPC/E and 2.180D for the TIP4P potential ( $1\text{D} = 3.335 \times 10^{-30} \text{ Cm}$ );  $\epsilon_0$  is the dielectric constant of the vacuum. The calculated results are shown in Fig. 5. The surface potentials for the SPC/E and TIP4P models are  $-0.58 \text{ V}$  and  $-0.39 \text{ V}$  at 293 K, respectively. Compared with the value of  $-0.55 \text{ V}$  reported by Zakharov *et al.* [5] at 300 K using the TIP4P, the present TIP4P results are large, which is relevant to the definition of surface potential. In Zakharov *et al.*'s simulation [5], the surface potential consists of dipolar and quadrupolar contributions, whereas only dipolar contribution is taken into account in this work. The absolute values of the surface potential show an increasing tendency with the decrease of temperature. If the surface potential is regarded as a linear function of temperature in the simulation temperature range, its temperature coefficients ( $d\chi/dT$ ) are equal to 13 and 12 mV/K for the SPC/E and TIP4P potentials respectively. The values have opposite sign to Schiffin's measurement [21]. In fact, the surface potential has great uncertainty in experiments and simulations, and even the results vary signs, which is induced by the measure method, potential function and calculation technique. As few experimental results can be obtained in the supercooled region to test the simulations, our aim is only to provide calculated values to predict the surface potential of supercooled water. In addition, the surface potential-temperature curves display a flat near 273 K as illustrated in Fig. 5. Whether this behavior corresponds to a transition of molecular structure near surface or is relevant to the second inflection point of the surface tension is still not clear. The absolute values of the surface potential for the SPC/E model are always larger than that for the TIP4P, which is consistent with the above analyses about orientation distribution of surface molecules and the result of the molecular structure determined by potential models.



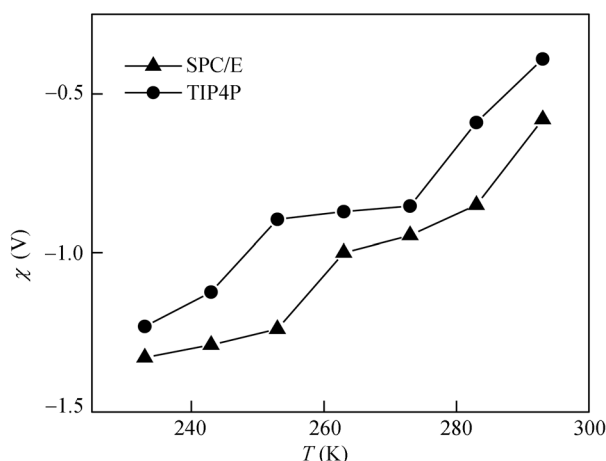


Fig. 5. Surface potentials of supercooled water as a function of temperature. The triangles and squares are results for the SPC/E and TIP4P potentials respectively.

### 3 Conclusions

MD simulations are accomplished to study the surface properties of supercooled water from 228 to 293 K. For the SPC/E potential, the simulated surface tension agrees well with the experimental results. Moreover, the temperature dependence of the surface tension for both the SPC/E and TIP4P potentials tends to increase in the supercooled region, which is consistent with the experiments. The simulated orientational structure of water molecules indicates that there exists the orientational ordering near the surface. The calculated surface potential displays negative value and positive temperature coefficient. Combined with the above results, the SPC/E potential reproduces accurately the surface tension, causes stronger orientational ordering of water molecules near the surface, and gives a better description of the surface properties of supercooled water.

**Acknowledgements** This work is financially supported by the National Natural Science Foundation of China (Grant Nos. 50121101, 50395105 and 50271058), and the Doctorate Foundation of Northwestern Polytechnical University. The authors would like to thank the Center for High Performance Computation of Northwestern Polytechnical University.

### References

- Basu J K, Hazra S, Sanyal M K. Growth mechanism of Langmuir-Blodgett films. *Phys Rev Lett*, 1999, 82: 4675–4678[DOI]
- Taylor R S, Shields R L. Molecular-dynamics simulations of the ethanol liquid-vapor interface. *J Chem Phys*, 2003, 119: 12569–12576[DOI]
- Velev O D, Gurov T D, Ivanov I B, et al. Abnormal thickness and stability of nonequilibrium liquid films. *Phys Rev Lett*, 1995, 75: 264–267[DOI]
- Weng J G, Park S, Lukes J R, et al. Molecular dynamics investigation of thickness effect on liquid films. *J Chem Phys*, 2000, 113: 5917–5923[DOI]
- Zakharov V V, Brodskaya E N, Laaksonen A. Surface tension of water droplets: A molecular dynamics study of model and size dependencies. *J Chem Phys*, 1997, 107: 10675–10683[DOI]

- 6 Wang J Z, Chen M, Guo Z Y. A two-dimensional molecular dynamics simulation of liquid-vapor nucleation. *Chin Sci Bull*, 2003, 48(7): 623–626
- 7 Guissani Y, Guillot B. A computer simulation study of the liquid-vapor coexistence curve of water. *J Chem Phys*, 1993, 98: 8221–8235[DOI]
- 8 Wilson M A, Pohorille A, Pratt L R. Surface potential of the water liquid-vapor interface. *J Chem Phys*, 1988, 88: 3281–3285[DOI]
- 9 Alejandre J, Tildesley D J, Chapela G A. Molecular dynamics simulation of the orthobaric densities and surface tension of water. *J Chem Phys*, 1995, 102: 4574–4583[DOI]
- 10 Matsumoto M, Kataoka Y. Study on liquid-vapor interface of water (I): Simulation results of thermodynamic properties and orientational structure. *J Chem Phys*, 1988, 88: 3233–3245[DOI]
- 11 Floriano M A, Angell C A. Surface tension and molar surface free energy and entropy of water to  $-27.2^{\circ}\text{C}$ . *J Phys Chem*, 1990, 94: 4199–4202[DOI]
- 12 Jorgensen W L, Chandrasekhar J, Madura J D. Comparison of simple potential functions for simulating liquid water. *J Chem Phys*, 1993, 79: 926–935[DOI]
- 13 Berendsen H J C, Grigera J R, Straatsma T P. The missing term in effective pair potentials. *J Phys Chem*, 1987, 91: 6269–6271[DOI]
- 14 Arbuckle B W, Clancy P. Effects of the Ewald sum on the free energy of the extended simple point charge model for water. *J Chem Phys*, 2002, 116: 5090–5098[DOI]
- 15 Tarazona P, Chacon E, Reinaldo-Falagan M, et al. Layering structures at free liquid surfaces: The Fisher-Widom line and the capillary waves. *J Chem Phys*, 2002, 117: 3941–3950[DOI]
- 16 Schwartz D K, Scholssman E K, Kellogg G J, et al. Thermal diffuse X-ray-scattering studies of the water-vapor interface. *Phys Rev A*, 1990, 41: 5687–5690[DOI]
- 17 Nijmeijer N J P, Bakker A F, Bruin C, et al. A molecular dynamics simulation of the Lennard-Jones liquid-vapor interface. *J Chem Phys*, 1988, 89: 3789–3792[DOI]
- 18 Vargaftik N B, Volkov B N, Voljak L D. International tables of the surface tension of water. *J Phys Chem Ref Data*, 1983, 12: 817–820
- 19 Pellicer J, Garcia-Morales V, Guanter L, et al. On the experimental values of the water surface tension used in some textbook. *Am J Phys*, 2002, 79: 705–709[DOI]
- 20 Leyendekkers J V, Hunter R J. Thermodynamic properties of water in the subcooled region. *J Chem Phys*, 1982, 82: 1447–1453[DOI]
- 21 Schiffrin D J. Real standard entropy of ions in water. *Trans Faraday Soc*, 1970, 66: 2464–2468